Materials Science and Engineering A 528 (2011) 8694–8699

Contents lists available at SciVerse ScienceDirect

Materials Science and Engineering A

journal homepage: www.elsevier.com/locate/msea

The effect of impurity level on ultrafine-grained microstructures and their stability in low stacking fault energy silver☆

Zoltán Hegedűs[a], Jenő Gubicza[a,*], Megumi Kawasaki[b], Nguyen Q. Chinh[a], Zsolt Fogarassy[c], Terence G. Langdon[b,d]

[a] Department of Materials Physics, Eötvös Loránd University, Pázmány Péter s. 1/A. H-1117 Budapest, Hungary
[b] Departments of Aerospace & Mechanical Engineering and Materials Science, University of Southern California, Los Angeles, CA 90089-1453, USA
[c] Research Institute for Technical Physics and Materials Science, P.O. Box 49, H-1525 Budapest, Hungary
[d] Materials Research Group, School of Engineering Sciences, University of Southampton, Southampton SO17 1BJ, UK

ARTICLE INFO

Article history:
Received 4 July 2011
Received in revised form 18 August 2011
Accepted 21 August 2011
Available online 26 August 2011

Keywords:
Severe plastic deformation
Equal-channel angular pressing
Silver
Stacking fault energy
Thermal stability

ABSTRACT

The effect of impurity content on the evolution of microstructure in low stacking fault energy silver processed by severe plastic deformation (SPD) was studied. The SPD-processing was carried out on 4N5 and 4N purity Ag samples by equal-channel angular pressing (ECAP) up to 16 passes. It was found that, although the minimum grain size and the maximum dislocation density were not affected by the different impurity atom content, there is a lower degree of twinning in the less pure material for high number of passes. The small increase of impurity level from 4N5 to 4N in Ag resulted in a significantly better thermal stability at room temperature for the ultrafine-grained microstructures obtained by ECAP.

1. Introduction

Contamination- and porosity-free bulk ultrafine-grained (UFG) materials can be processed by severe plastic deformation (SPD) [1–4]. One of the most frequently used method of SPD is equal-channel angular pressing (ECAP) [2,4]. The long-term stability of the ECAP-processed UFG microstructures is an important factor in their industrial applications. The question of stability is emerging not only in high-temperature applications but even during storage at room temperature (RT). Recent reports [5–8] have shown that pure UFG Cu and Ag samples exhibited self-annealing after ECAP-processing when they were stored at RT. Self-annealing was also observed in Cu, Au and Ag [9,10] processed by high-pressure torsion (HPT). For the same purity level, the self-annealing was faster for Ag than for Cu. This can be explained by the very low stacking fault energy (SFE) of Ag among face centered cubic (fcc) metals that results in a high degree of dislocation dissociation. The annihilation of highly dissociated dislocations is difficult during ECAP, yielding a very high dislocation density that increases the driving force for recovery and recrystallization in the samples during the subsequent storage. Additionally, the very low twin boundary energy in Ag (~8 mJ/m^2 [11]) facilitates the nucleation of new defect-free grains bounded by twin boundaries that results in an easier recrystallization of the ECAP-processed specimens. It is noted that in 5N purity Al having high SFE recrystallization was observed even during ECAP processing at RT due to its low melting point and very high purity level [12].

It is generally accepted that the impurity content is an important factor either in the development of the UFG microstructure during SPD or in its thermal stability. Since the solute atoms hinder the motion of lattice defects, such as dislocations and grain boundaries, they therefore stabilize the UFG microstructure. The effect of impurity concentration on the thermal stability of medium or high stacking fault energy fcc metals (e.g. Ni and Cu) processed by SPD has been studied in the literature [13,14]. In the case of Ni processed by high-pressure torsion, calorimetry studies revealed only minor differences between the high temperature stability of 4N and 4N8 purity samples [13,14]. At the same time, in ECAP-processed 5N purity Cu stored at RT the recrystallization starts much earlier (two months after ECAP) than in 3N6 purity Cu samples (8 years) [5,7]. There is also a report of the strong effect of impurity concentration on partial recrystallization in a thin wire-drawn Cu [15]. However, to the knowledge of the authors, the effect of the change of solute atom concentration on the evolution of the microstructure in high purity Ag during ECAP and its thermal stability has not

☆ Dedicated to Prof. Michael Zehetbauer on the occasion of his 60th birthday.
* Corresponding author. Tel.: +36 1 372 2876; fax: +36 1 372 2811.
E-mail address: gubicza@metal.elte.hu (J. Gubicza).

0921-5093/$ – see front matter © 2011 Elsevier B.V. All rights reserved.
doi:10.1016/j.msea.2011.08.034

Table 1
The chemical composition of 4N and 4N5 purity samples: the concentration values supplied by the manufacturers are given in ppm.

4N5	Cu	Pb	Fe	Se	Ir	Au	Pd
	13	14	5	6	6	10	2
4N	Cu	Pb	Fe	Se	Sb	Bi	
	30	10	10	10	10	20	

been investigated. In a recent report [8], the microstructure and its self-annealing in 4N5 purity Ag were studied as a function of the number of ECAP passes. In this paper, the evolution of microstructure and its stability for 4N purity ECAP-processed Ag are presented and compared with the characteristics of 4N5 purity counterparts. The thermal stability is studied during storage at RT for different numbers of passes between 1 and 16.

2. Experimental materials and procedures

Samples of silver of 99.99 at.% (4N) and 99.995% (4N5) purity (alloying elements and their concentrations are listed in Table 1) were manufactured by American Elements and ESPI Metals, respectively. For both compositions, billets having lengths of ~70 mm and diameters of 10 mm were annealed at 741 K for 1 h. This temperature corresponds to 0.6 T_m, where T_m is the absolute melting point of Ag. The annealed samples were processed through 1, 4, 8 and 16 passes of ECAP at RT with a pressing velocity of 8 mm s^{-1}. The pressing was conducted using route B_c where the billet is rotated in the same sense by 90° about its longitudinal axis after each pass [16]. The ECAP die had an internal channel angle of 90° and an outer arc of curvature of 20°. In this configuration one pass corresponds to an equivalent strain of ~1 [17].

Microstructures were examined by X-ray line profile analysis on transverse sections cut perpendicular to the axes of the billets. The measurements of the X-ray diffraction lines were performed using a special high-resolution diffractometer (Nonius FR591) with CuKα_1 radiation (λ = 0.15406 nm). The line profiles were evaluated using the extended Convolutional Multiple Whole Profile (eCMWP) fitting procedure [18,19]. In this method, the diffraction pattern is fitted by the sum of a background spline and the convolution of the instrumental pattern and the theoretical line profiles related to the crystallite size, dislocations and twin faults. The details of the eCMWP procedure are available elsewhere. [18,19]. This method gives the dislocation density and the twin-boundary frequency with good statistics, where the twin-boundary frequency is defined as the fraction of twin boundaries among the {1 1 1} lattice planes. The grain structure was examined using a Philips CM-20 transmission electron microscope (TEM) operating at 200 kV. The TEM samples were mechanically thinned to ~80 μm, cooled to liquid nitrogen temperature and then thinned with 6 keV Ar^+ ions from both sides until perforation. Finally, a thin damaged layer was removed using 2 keV Ar^+ ions.

The hardness of the samples was measured using a Zwick Roell ZHμ Vickers microhardness indenter with an applied load of 2000 mN and a dwell time of 10 s. The deformation behavior was studied using uniaxial compression testing with a computer-controlled hydraulic mechanical testing MTS 810 machine. For all

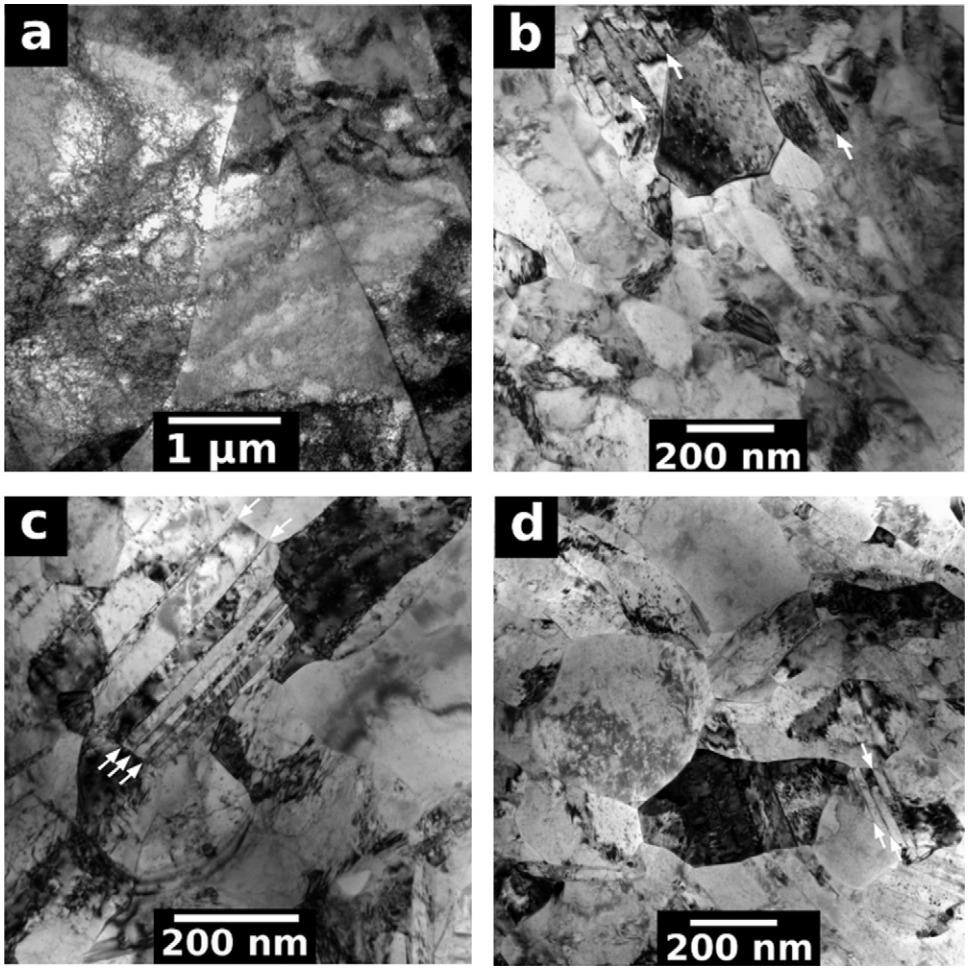

Fig. 1. TEM images showing the microstructures of 4N purity Ag after (a) 1, (b) 4, (c) 8 and (d) 16 passes of ECAP: examples of twin boundaries are indicated by white arrows.

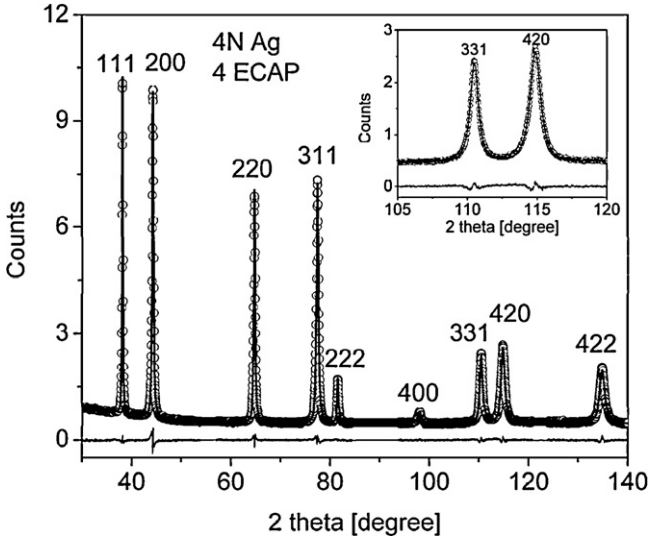

Fig. 2. A fitted X-ray diffraction pattern for 4N Ag processed by 4 passes: the open circles and the solid line represent the measured data and the fitted curves, respectively. The difference between the measured and fitted patterns is also shown at the bottom of the figure.

of these tests, the direction of compression was parallel to the longitudinal axis of each billet.

The samples were stored at RT and hardness testing as well as X-ray line profile analysis were performed monthly in order to monitor the self-annealing of the samples.

3. Results and discussion

3.1. Effect of impurities on the evolution of microstructure during ECAP processing

The values of the mean grain size were ~56 μm and ~20 μm in the initial state and after one pass of ECAP, respectively, for 4N purity Ag as determined by scanning electron microscopy. Fig. 1 shows the TEM images of the microstructures of 4N purity Ag after different numbers of passes in ECAP corresponding to (a) 1 pass, (b) 4 passes, (c) 8 passes and (d) 16 passes. Inside the grains the dislocation density was high as revealed by the TEM image in Fig. 1a. Fig. 1b shows that the mean grain size after 4 passes decreased to ~230 nm and further ECAP deformation gave only a slight additional grain refinement. After 8 and 16 passes the mean grain size values were ~220 and ~200 nm, respectively, as shown in Fig. 1c and d. The evolution of the grain structure in 4N5 purity Ag as a function of number of ECAP passes was presented earlier [8] (the notation of 4N purity was a misprint in that paper). The mean grain size in 4N5 purity Ag between 4 and 16 passes was also ~200 nm indicating that the two times larger impurity content in the present case did not affect significantly the minimum grain size achievable by ECAP.

The dislocation density and the twin boundary frequency were determined by X-ray line profile analysis. As an example, Fig. 2 shows the fitted pattern for 4N Ag processed by 4 passes. The open circles and the solid line represent the measured data and the fitted curves, respectively. The difference between the measured and fitted patterns is also shown at the bottom of the figure. The dislocation density and the twin boundary frequency are plotted as a function of the number of ECAP passes for 4N5 and 4N purity Ag in Fig. 3. For both series, the evolution of the dislocation density was similar, increasing up to 8 passes and then decreasing. For 1 pass the dislocation density was larger for 4N purity Ag ($26 \pm 4 \times 10^{14}\ m^{-2}$) than for the more pure 4N5 sample ($16 \pm 2 \times 10^{14}\ m^{-2}$). Gallagher

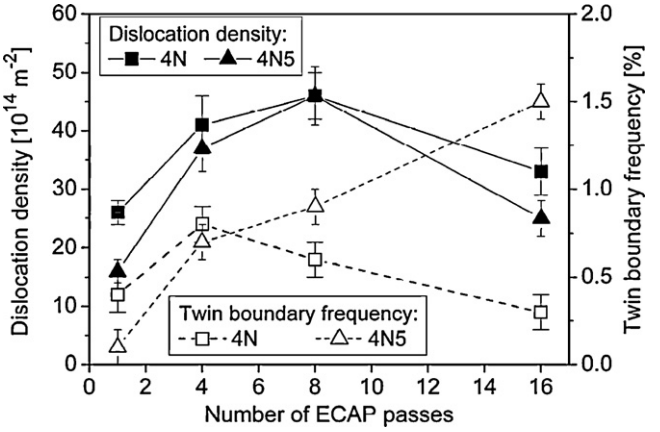

Fig. 3. The variation of the dislocation density and the twin boundary frequency with the number of ECAP passes for 4N5 and 4N purity Ag.

[20] has shown that both the impurities and solid solution alloying reduce SFE in Ag. As for small impurity contents, the relative change of SFE has the same order of magnitude as the impurity concentration [20], therefore in the present materials where these concentrations are not more than 10^{-4} the reduction of SFE due to contamination is marginal. As a consequence, the equilibrium splitting distances calculated for screw (2.5 nm) and edge dislocations (6.3 nm) in pure Ag [8] can be used for both 4N and 4N5 purity samples. The high degree of dislocation dissociation due to low SFE hinders dislocation annihilation, leading to a large dislocation density even after the first pass of ECAP. As this effect is similar for the two compositions, the larger dislocation density in 4N Ag after 1 pass can be explained solely by the stronger pinning effect of the larger concentration of impurities that hinders dislocation annihilation. Furthermore, the interaction force between dislocations and solute atoms is proportional to the square of the difference of the solute and solvent atomic sizes [21]. Therefore, according to Table 1, the most effective pinning atoms are Pb, Bi and Sb in the present Ag samples. The fractions of these elements in the overall impurity content are 44% and 25% for 4N and 4N5 samples, respectively, therefore the pinning effect of impurities on dislocations is much higher in 4N Ag compared to 4N5 sample than suggested by the difference in the total impurity concentrations.

In addition to dislocation glide, twinning also contributes to plastic deformation for both impurity levels. In the TEM images of Fig. 1 some twin boundaries are indicated by white arrows. The twin sources are usually located at dislocation glide obstacles such as Lomer–Cottrell locks or grain boundaries where the local stress exceeds the critical stress needed for twin nucleation [22]. The larger dislocation density in 4N purity Ag processed by 1 pass increases the number of twin nucleation sites at glide obstacles, thereby leading to a higher twin boundary frequency than in 4N5 Ag.

For both impurity contents, the dislocation density increased with increasing number of passes and saturated after 8 passes with a very large value of $46 \pm 5 \times 10^{14}\ m^{-2}$ as compared to other pure fcc metals processed by ECAP at RT: for example the report by Schafler et al. [23]. This large dislocation density can be attributed to the retarded annihilation due to the high degree of dislocation dissociation. After 8 passes of ECAP, the grain size is reduced to 200 nm and the majority of impurities are most probably segregated at the grain boundaries as was shown for other UFG materials [24]. As a consequence, there is a reduction in the difference between the impurity concentrations along dislocations inside the grains in 4N5 and 4N samples that leads to similar saturation dislocation densities for the two compositions. In addition to cross-slip and climb, twinning also contributes to the annihilation of dislocations as the

lattice dislocations are dissociated into twinning partials at glide obstacles and a twin forms by slipping of these partials in neighboring {1 1 1} lattice planes [25–28]. As the twin boundaries obstruct the activity of dislocation glide sources [22], therefore the thermally activated annihilation and the dissociation due to twinning give a reduction in the dislocation density in Ag between 8 and 16 passes. A similar decrease of the dislocation density due to dynamic recovery was observed also in Cu processed by more than 8 passes in ECAP [29].

After 4 passes the evolution of the twin boundary frequency is different for 4N5 and 4N samples (see Fig. 3). In the former case, the twin boundary frequency increases monotonously up to 16 passes while for 4N specimens it decreases slightly after 8 passes. As was noted, after 4 passes the grain size was reduced to ~200 nm and, due to the large number of grain boundaries, the twins are mainly nucleated at the grain boundaries as was already observed for other nanomaterials [30]. The impurities and the alloying atoms in solid solution are usually segregated at grain boundaries during SPD at RT [24]. As a consequence, the higher impurity content in 4N Ag hinders the nucleation of twins at grain boundaries. The interaction of dislocations and twins give untwining inside the grains [22], therefore the reduced activity of twin sources at the grain boundaries in 4N purity Ag leads to a significant decrease in the total twin boundary frequency after 16 passes. Between 8 and 16 passes, the lower twin formation rate in 4N purity Ag contributes to the smaller reduction of the dislocation density compared to the 4N5 purity material.

Recent studies [31,32] on 4N purity Al and Al–1% Mg alloy have shown that the fraction of low-angle grain boundaries decreases with increasing the number of ECAP passes in both materials, but its minimum value in Al–1% Mg (~35%) is higher than that for pure Al (~25%). This can be explained by the dragging effect of impurities on dislocations that hinders the evolution of low-angle grain boundaries into high-angle boundaries. The higher alloying element concentration in Al–1% Mg also yielded a smaller grain size, ~700 nm, than in pure Al, ~1.3 μm, as determined by electron backscatter diffraction (EBSD). The application of EBSD for the present 4N and 4N5 Ag samples processed by ECAP was unsuccessful since the resolution of this method, ~100 nm, is close to the grain size (~200 nm). In practice, the higher impurity content in 4N Ag is expected to yield a larger low-angle grain boundary fraction than for 4N5 Ag. However, this effect is most probably less pronounced than for Al and Al–1% Mg due to the smaller difference between the impurity contents in the present Ag samples.

The stress–strain data obtained in compression for the 4N purity material are plotted in Fig. 4: similar results were also presented for 4N5 Ag earlier [8]. The initial sample has a yield strength of 25 MPa and exhibits a strong strain hardening. After 1 pass the compression stress–strain curve shows only a weak work hardening with a flow stress of ~275 MPa and this increases to ~336 MPa after 4 and 8 passes. Between 8 and 16 passes the flow stress decreases to ~314 MPa in accordance with the decrease in both the dislocation density and the twin boundary frequency.

3.2. Effect of impurities on self-annealing during storage at room temperature

It was shown earlier [8] that 4N5 purity Ag samples processed by 4–16 ECAP passes will self-anneal during storage at RT leading to a decrease in the hardness of the material. Fig. 5a plots the hardness as a function of storage time for 4N5 purity Ag processed by different numbers of passes. After 1 pass, the hardness remained unchanged showing that neither recovery nor recrystallization occurred: this is also confirmed by TEM and X-ray measurements [8]. The evolution of hardness with storing time revealed a self-annealing after 4, 8 and 16 passes of ECAP. After 4 months of storage the hardness of the samples processed by 8 and 16 passes approached the value characteristic of a well-annealed sample before ECAP. The larger the number of passes, the faster the hardness reduction. Up to 8 passes this phenomenon can be explained by the increase in the defect densities (grain boundaries, dislocations, twin faults) with increasing numbers of passes that gives a higher

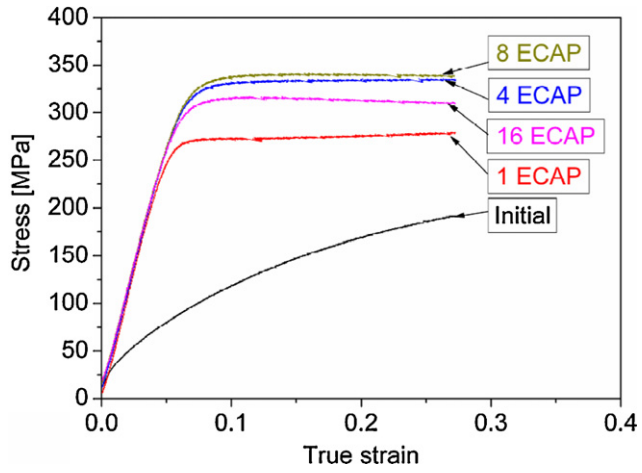

Fig. 4. True stress–true strain curves obtained on 4N purity samples immediately after ECAP for different numbers of passes: a curve for the initial unpressed condition is also shown.

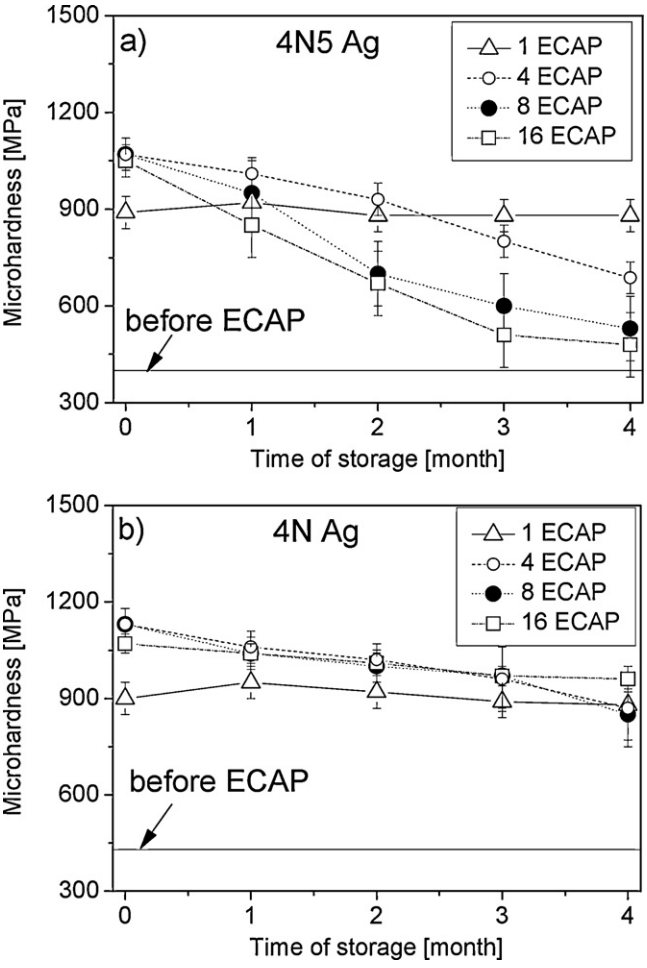

Fig. 5. Values of the microhardness after processing by ECAP for 1, 4, 8 and 16 passes as a function of the storage time at room temperature for (a) 4N5 and (b) 4N purity Ag.

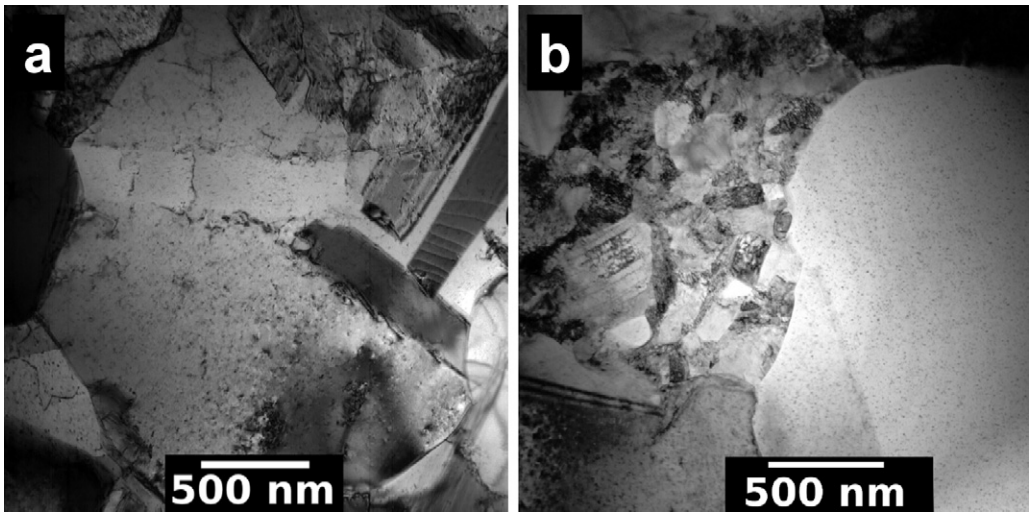

Fig. 6. Bright TEM images showing the microstructures of (a) the 4N5 purity sample processed through 8 ECAP passes and stored at room temperature for 4 months and (b) the 4N purity specimen after 8 ECAP passes and storage for 1 year.

driving force for annealing processes. Previous X-ray line profile analysis and TEM investigations [8] revealed that both recovery and recrystallization occurred during self-annealing in ECAP-processed 4N5 purity Ag. It was found that, despite the lower dislocation density after 16 passes, the recrystallization was faster than after 4 or 8 passes. This can be explained by the larger twinning activity, as in the volumes where the twin boundary frequency increased at the expense of the dislocation density, the stored energy decreased due to the very low twin boundary energy of Ag. Thus, these volumes can act as nuclei for the new grains formed by recrystallization thereby reducing the time required for grain nucleation in the 4N5 Ag sample processed by 16 passes. This is consistent with observations that the nuclei of recrystallized grains form primarily at deformation twins in low stacking fault energy metals [33].

The hardness as a function of storage time for 4N purity samples is shown in Fig. 5b. The two times higher impurity content in 4N specimens yielded a considerably better stability in the UFG Ag samples produced by ECAP compared to the 4N5 purity specimens. The hardness of the sample processed by 1 pass remained unchanged within the experimental error similar to the case of higher purity material. At the same time, and contrary to the 4N5 material, the hardness of 4N purity Ag specimens after 4, 8 and 16 passes did not fall below the value obtained after 1 pass. The much better stability of the UFG microstructure in the less pure samples is confirmed by a comparison of the TEM images of Fig. 6 taken on specimens processed by 8 passes and stored at RT. Fig. 6a shows that in the 4N5 purity sample only fully recrystallized volumes are detected after 4 months of storage while in the 4N purity specimen the remaining ultrafine-grained regions are also observed even after 1 year of storage as illustrated in Fig. 6b. The higher stability of the ECAP-processed 4N purity samples can be attributed to the larger impurity content that retards recovery and recrystallization processes during storage of the samples. A recent study of annealing in Cu processed by ECAP showed that recrystallization occurs first in regions where grain boundaries have high angles of misorientation [34]. Since the angle of misorientation at grain boundaries is expected to be higher for the more pure metal, it is reasonable to anticipate that this effect contributes to the lower stability of 4N5 Ag.

According to the hardness tests, in the 4N Ag material the slowest self-annealing was detected for the sample processed by 16 passes and that is an essentially different behavior from that observed for the 4N5 material. Fig. 7 presents a visual confirmation of this difference where there is a comparison between the

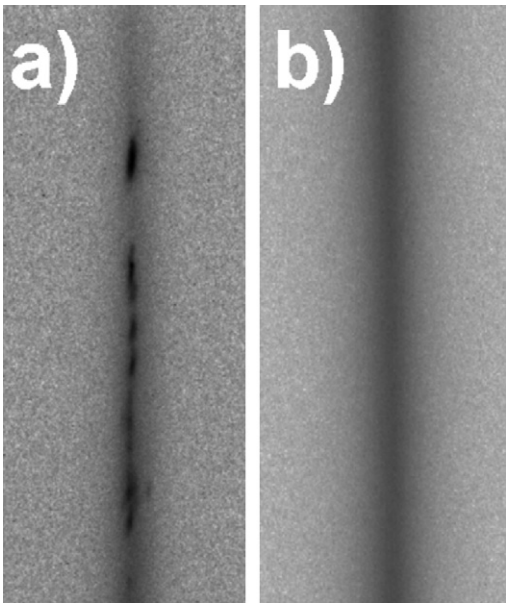

Fig. 7. Debye–Scherrer diffraction rings for the 311 reflection of X-rays in (a) 4N5 and (b) 4N purity samples after 16 ECAP passes and storage at room temperature for 4 months.

311 X-ray Debye–Scherrer diffraction rings obtained for (a) 4N5 and (b) 4N Ag samples processed by 16 passes and stored at RT for 4 months. In Fig. 7a the intensity spots on the ring for the 4N5 purity sample correspond to recrystallized grains. The lack of these spots in Fig. 7b indicates that there is no strong recrystallization in the 4N purity specimen. The high stability against self-annealing in the case of the 4N purity Ag sample processed by 16 passes can be explained by the relatively low twin boundary frequency that reduces the number of locations where recrystallization occurs easily.

According to our earlier investigations on 4N5 purity UFG Ag [8], it appears that a relatively low total strain should be applied in the SPD-processing of pure, low SFE metals in order to avoid any significant strength degradation during their service lifetime. The present results suggest, in addition, that for a slightly higher impurity content the stability is a non-monotoneous function of the strain and a reasonably stable UFG microstructure with high strength may be achieved at very high strains of SPD. It is planned

to extend the study of self-annealing in low SFE Ag to even higher impurity contents.

4. Summary and conclusions

1. The minimum grain size achieved by ECAP at RT in pure Ag was ~200 nm irrespective of the impurity atom concentration. The dislocation density also showed similar evolution for both 4N5 and 4N impurity levels: first it increased and saturated after 8 passes at similar values and then decreased. At the same time, the evolution of twin boundary frequency was very different for the two impurity concentrations: it increased monotonously up to 16 passes in the case of 4N5 purity samples while for 4N purity specimens it saturated after 4 passes and then decreased with increasing number of passes. It appears that the impurity atoms are probably concentrated preferentially at the grain boundaries with decreasing grain size thereby hindering the emission of twinning partials from boundaries that leads to a decrease of the twinning activity in the less pure material.
2. The samples processed for 4–16 passes showed self-annealing during storage at RT. Despite the small difference in purity, the 4N samples exhibited a much lower degree of softening than 4N5 specimens as impurity atoms pinned dislocations and grain boundaries thereby hindering both recovery and recrystallization. In the case of the 4N5 purity samples, an increasing number of ECAP passes leads to more rapid self-annealing due to the increase in the twinned volumes that can act as nuclei for recrystallization. At the same time, the 4N purity specimen processed through 16 passes exhibited lower softening than the samples processed through 4 or 8 passes and this is due to the lower level of twinning.

Acknowledgements

This work was supported in part by the Hungarian Scientific Research Fund, OTKA, Grant No. K-81360, in part by the National Science Foundation of the United States under Grant No. DMR-0855009 (MK and TGL) and in part by the European Research Council under ERC Grant Agreement No. 267464-SPDMETALS (TGL). The European Union and the European Social Fund have provided financial support to this project under Grant Agreement No. TÁMOP 4.2.1./B-09/1/KMR-2010-0003. The authors thank Andrea Jakab for preparation of the TEM samples.

References

[1] R.Z. Valiev, R.K. Islamgaliev, I.V. Alexandrov, Prog. Mater. Sci. 45 (2000) 103–189.
[2] R.Z. Valiev, T.G. Langdon, Prog. Mater. Sci. 51 (2006) 881–981.
[3] A.P. Zhilyaev, T.G. Langdon, Prog. Mater. Sci. 53 (2008) 893–979.
[4] R. Kuzel, M. Janecek, Z. Matej, J. Cizek, M. Dopita, O. Srba, Metall. Mater. Trans. A 41 (2010) 1174–1190.
[5] G. Wang, S.D. Wu, L. Zuo, C. Esling, Z.G. Wang, G.Y. Li, Mater. Sci. Eng. A 346 (2003) 83–90.
[6] Y. Estrin, N.V. Isaev, S.V. Lubenets, S.V. Malykhin, A.T. Pugachov, V.V. Pustovalov, E.N. Reshetnyak, V.S. Fomenko, L.S. Fomenko, S.E. Shumilin, M. Janecek, R.J. Hellmig, Acta Mater. 54 (2006) 5581–5590.
[7] O.V. Mishin, A. Godfrey, Metall. Mater. Trans. A 39A (2008) 2923–2930.
[8] J. Gubicza, N.Q. Chinh, J.L. Lábár, Z. Hegedűs, T.G. Langdon, Mater. Sci. Eng. A 527 (2010) 752–760.
[9] H. Matsunaga, Z. Horita, Mater. Trans. 50 (2009) 1633–1637.
[10] J. Gubicza, S.V. Dobatkin, E. Khosravi, A.A. Kuznetsov, J.L. Lábár, Mater. Sci. Eng. A 528 (2011) 1828–1832.
[11] J.P. Hirth, J. Lothe:, Theory of Dislocations, Wiley, New York, 1982.
[12] W. Skrotzki, N. Scheerbaum, C.-G. Oertel, H.-G. Brokmeier, S. Suwas, L.S. Tóth, Acta Mater. 55 (2007) 2211–2218.
[13] D. Setman, E. Schafler, E. Korznikova, M.J. Zehetbauer, Mater. Sci. Eng. A 493 (2008) 116–122.
[14] D. Setman, M.B. Kerber, E. Schafler, M.J. Zehetbauer, Metall. Mater. Trans. A 41 (2010) 810–815.
[15] J. Schamp, B. Verlinden, J. Van Humbeeck, Scripta Mater. 34 (1996) 1667–1672.
[16] M. Furukawa, Y. Iwahashi, Z. Horita, M. Nemoto, T.G. Langdon, Mater. Sci. Eng. A 257 (1998) 328–332.
[17] Y. Iwahashi, J. Wang, Z. Horita, M. Nemoto, T.G. Langdon, Scripta Mater. 35 (1996) 143–146.
[18] G. Ribárik, J. Gubicza, T. Ungár, Mater. Sci. Eng. A 387–389 (2004) 343–347.
[19] L. Balogh, G. Ribárik, T. Ungár, J. Appl. Phys. 100 (2006) 023512.
[20] P.C.J. Gallagher, Metall. Trans. 1 (1970) 2429–2461.
[21] S.G. Song, J.S. Vetrano, S.M. Bruemmer, Mater. Sci. Eng. A 232 (1997) 23–30.
[22] P. Müllner, C. Solenthaler, Mater. Sci. Eng. A 230 (1997) 107–115.
[23] E. Schafler, G. Steiner, E. Korznikova, M. Kerber, M.J. Zehetbauer, Mater. Sci. Eng. A 410–411 (2005) 169–173.
[24] P.V. Liddicoat, X.-Z. Liao, Y. Zhao, Y. Zhu, M.Y. Murashkin, E.J. Lavernia, R.Z. Valiev, S.P. Ringer, Nat. Commun. 1 (2010) 63.
[25] J.A. Venables, Philos. Mag. 6 (1961) 379–396.
[26] J.B. Cohen, J. Weertman, Acta Metall. 11 (1963) 996–998.
[27] Y.T. Zhu, X.Z. Liao, S.G. Srinivasan, E.J. Lavernia, J. Appl. Phys. 98 (2005) 034319.
[28] Z.W. Wang, Y.B. Wang, X.Z. Liao, Y.H. Zhao, E.J. Lavernia, Y.T. Zhu, Z. Horita, T.G. Langdon, Scripta Mater. 60 (2009) 52–55.
[29] F. Dalla Torre, R. Lapovok, J. Sandlin, P.F. Thomson, C.H.J. Davies, E.V. Pereloma, Acta Mater. 52 (2004) 4819–4832.
[30] Y.T. Zhu, X.L. Wu, X.Z. Liao, J. Narayan, S.N. Mathaudhu, L.J. Kecskés, Appl. Phys. Lett. 95 (2009) 031909.
[31] M. Kawasaki, Z. Horita, T.G. Langdon, Mater. Sci. Eng. A 524 (2009) 143–150.
[32] C. Xu, Z. Horita, T.G. Langdon, Mater. Sci. Eng. A 528 (2011) 6059–6065.
[33] H. Paul, J.H. Driver, C. Maurice, A. Piatkowski, Acta Mater. 55 (2007) 575–588.
[34] O.V. Mishin, J.R. Bowen, Metall. Mater. Trans. A 40 (2009) 1684–1692.